The Main Builders of Mediterranean Coralligenous: 2D and 3D Quantitative Approaches for its Identification

Valentina Alice Bracchi[1,2]*, Pietro Bazzicalupo[1], Luca Fallati[1], Andrea Giulia Varzi[1], Alessandra Savini[1,2], Mauro Pietro Negri[1], Antonietta Rosso[2,3], Rossana Sanfilippo[2,3], Adriano Guido[4], Marco Bertolino[5], Gabriele Costa[1,5], Elena De Ponti[6], Riccardo Leonardi[3], Maurizio Muzzupappa[7] and Daniela Basso[1,2]

[1]Department of Earth and Environmental Sciences, University of Milano-Bicocca, Milano, Italy, [2]CoNISMa – Consorzio Nazionale Interuniversitario per le Scienze del Mare, Roma, Italy, [3]Department of Biological, Geological and Environmental Sciences, University of Catania, Catania, Italy, [4]Department of Biology, Ecology and Earth Sciences, University of Calabria, Cosenza, Italy, [5]Department of Earth, Environmental and Life Sciences (DISTAV), University of Genoa, Genoa, Italy, [6]Department of Medical Physics, ASST Monza, University of Milano-Bicocca, Monza, Italy, [7]Department of Mechanical, Energy and Management Engineering (DIMEG), University of Calabria, Cosenza, Italy

Along the Mediterranean Sea shelf, algal reefs made of crustose coralline algae and Peyssonneliales are known as Coralligenous. It ranks among the most important ecosystems in the Mediterranean Sea because of its extent, complexity, and heterogeneity, supporting very high levels of biodiversity. Descriptive approaches for monitoring purposes are often aimed at assessing the surficial ephemeral canopy, which is sustained and controlled by the occurrence of the long-lasting rigid structure at the base. This practice led to the non-univocal definition of Coralligenous, sometimes indicated as "animal Coralligenous" because of the surficial dominance of these components. The quantitative assessment of the builders that actively build up the persistent structure through geological time is therefore a fundamental topic. We collected two discrete coralligenous samples in front of Marzamemi village (Sicily, Ionian Sea), the first from an area of a dense coralligenous cover (- 37 m) and the second one from an area with sparse build-ups (- 36 m). By using image analysis and computerized axial tomography, we distinguished and quantified the different components both on the surface and inside the framework. In both cases, our results confirm the primary role of crustose coralline algae as major builders of the Mediterranean Coralligenous, this aspect matching with the evidence from the Quaternary fossil record. We suggest that the role of encrusting calcareous red algae in the Coralligenous should be considered in conservation and management policies.

Keywords: algal reef, bioconstruction, crustose coralline algae, framework, Marzamemi

1 INTRODUCTION

Encrusting calcareous red algae, among which are crustose coralline algae (CCA) and mineralized Peyssonneliales, are one of the key elements of the benthic marine shelf communities.

According to Fagerström (1991), who defined "builder" as any organism that builds a structure that survives to the death of the organism itself, encrusting calcareous red algae play a fundamental role as reef builders, being one of the most important components of the tropical coral reefs

(Littler, 1972). In recent revisions of the Mediterranean bioconstructions along the Italian coast, builder organisms have been indicated also as constructors (Rosso and Sanfilippo, 2009) or bioconstructors (Ingrosso et al., 2018). Furthermore, encrusting calcareous red algae are also able to develop endemic primary algal-dominated frameworks known as Coralligenous in the temperate waters of the Mediterranean Sea (e.g., Ballesteros, 2006). Coralligenous is considered an organic reef made of in-place reef-building organisms (Riding, 2002).

Marion (1883) first used the term *coralligène* (= @Coralligenous) while referring to the hard bottom found by anglers from Marseille (France), where *Corallium rubrum* (Linnaeus, 1758) was often found; Coralligenous literally means "producer of coral," relating to the abundance of this red coral. Pruvot (1894, 1895) and Feldmann (1937) studied the Coralligenous of Banyuls-sur-Mer (France) and first identified the main CCA genera and species responsible for the development of such frameworks. In the fifties and sixties, a fundamental contribution to our knowledge of the Mediterranean benthos came from the Endoume School (Marseille, France), summarized in the *Nouveau Manuel de Bionomie marine benthique de la Mer Méditerranée* by Pérès and Picard (1964). They defined the Coralligenous as the climax biocoenosis of the circalittoral zone, where CCA and mineralized Peyssonneliales develop primary or secondary hard bottoms of biogenic origin, under sciaphilous conditions. In addition to encrusting calcareous red algae, a contribution as builders of other organisms such as bryozoans, serpulids, and sponges has been sometimes indicated (Pérès and Picard, 1964; Pérès, 1982; Hong, 1982; Bellan-Santini et al., 1994; Ballesteros, 2006; Bertolino et al., 2017a, 2019; Costa et al., 2019).
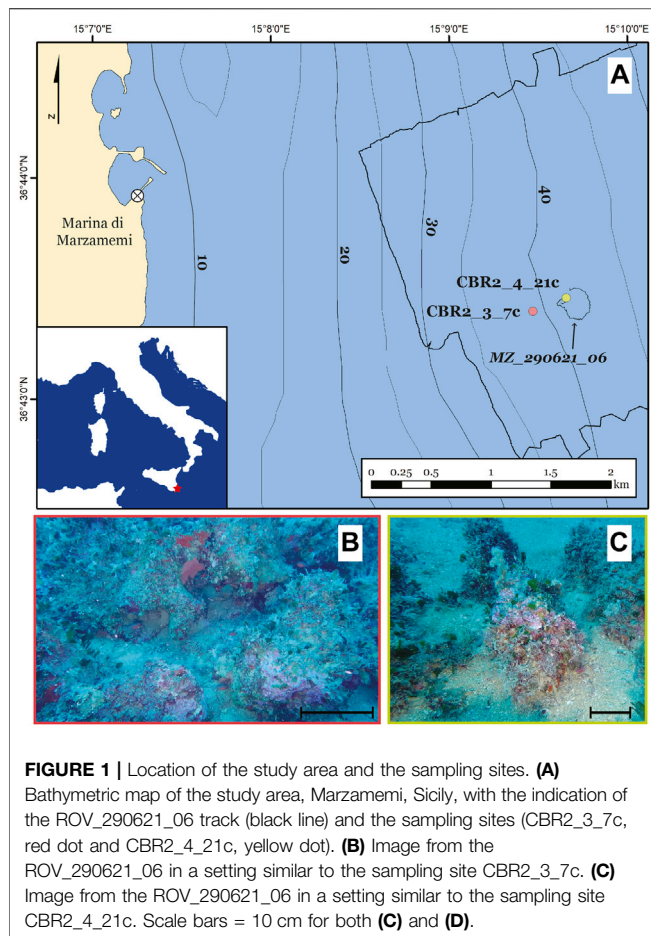
At the scale of geological time, the overgrowing of such algae along the shelves gives rise to a geomorphological unit (bank or discrete columns) which completely changes the nature of the seafloor substrate. In turn, coralligenous build-ups modify the seascape (Bracchi et al., 2015, 2017), increase the carbonate production (Marchese et al., 2020), and may be preserved in the fossil record (Bosence and Pedley 1982; Carannante and Simone 1996; Rasser 2000; Nalin et al., 2006; Basso et al., 2007, 2009; Titschack et al., 2008; Bracchi et al., 2014, 2016, 2019).

Despite this definition, there is currently no real consensus among the scientific community to give a unique definition of Coralligenous. Past and recent biocenotic studies have shown the structural complexity of this habitat and the difficulty of its precise definition. Owing to its heterogeneity, Coralligenous has been interpreted as an assembly of several communities rather than a single community (Ballesteros, 2006; La Rivière et al., 2021). Because of its extent and complexity, this habitat supports high levels of biodiversity (Ballesteros, 2006) and ranks among the most important ecosystems in the Mediterranean Sea. Moreover, its multi-scale crevices and cavities produced by the irregular growth of algal thalli and the destructive action of some boring organisms contribute to increasing its biodiversity (Laborel 1961; Laubier 1966; Sartoretto et al., 1996; Cerrano et al., 2001), among which sponges represent one of the most abundant taxa (Bertolino et al., 2013; Costa et al., 2019).

Pérès and Picard (1964) originally indicated the spatial heterogeneity of Coralligenous and its co-occurrence with other types of habitats. Ballesteros (2006) introduced the wording of "animal-dominated" Coralligenous to indicate circalittoral bioherms not apparently dominated by CCA and mineralized Peyssonneliales. Several authors, consequently, indicated the forests of the gorgonian *Paramuricea clavata* (Risso, 1826) as one of the most peculiar elements characterizing Mediterranean coralligenous (Musard et al., 2014; Ponti et al., 2018). Bertolino et al. (2017a), while studying the coralligenous of Porto Cesareo (Apulia, Italy), noted the presence of abundant tubes of the serpulid *Protula* sp. that contributed to the framework. Enrichetti et al. (2019) used the definition "coralligenous animal forest" to indicate a particular aspect of Coralligenous dominated by gorgonians. Corriero et al. (2019) reported the occurrence of a bioconstruction along the Apulian coast (Italy) mostly made up of scleractinians together with some auxiliary building species, while the contribution of the CCA appeared negligible. Chimienti et al. (2020) described a mesophotic black coral forest in the Adriatic Sea, settled on animal-dominated bioconstructions, which has been considered as Coralligenous despite the very scarce presence of CCA. A recent revision of the Mediterranean biocoenoses (La Rivière et al., 2021) indicated at least seven associations and five facies for the coralligenous biocoenosis, all characterizing the surficial canopy of the build-ups.

Understandably, all these findings, although undoubtedly increasing our knowledge on mesophotic reefs and provide detailed information about the canopy community, rarely address the nature of the biogenic substrate, namely, the bioherm supporting these surface communities. Nevertheless, physical builders (*sensu* Fagerström, 1991) play a crucial role in the long-term survival of the build-ups, and the identification and distinction of the role of specific taxa should be considered, together with the canopy communities.

Finally, direct and indirect human impacts and mass mortality events threaten coralligenous, affecting the stability of this precious ecosystem and, thus, strongly compromising its conservation because of its destruction and reduction of biodiversity (Ingrosso et al., 2018). Due to its critical importance, Coralligenous is listed among Mediterranean priority habitats by the EU Habitats Directive and included in the network of Natura 2000 sites (92/43/CE). It is also subject to specific conservation plans in the framework of the Barcelona Convention (UNEP-MAP-RAC/SPA, 2008; UNEP-MAP-RAC/SPA, 2017). Coralligenous is included among the habitats monitored under the Marine Strategy Framework Directive (MSFD, EC, 2008). Consequently, non-destructive approaches have been developed to assess the ecological quality and health status of coralligenous assemblages. Most of them are based on visual census methods (Remotely Operated Vehicle, ROV, photo-transects or quadrats by scuba divers) (Kipson et al., 2011; Deter et al., 2012; Zapata-Ramírez et al., 2013; Cecchi et al., 2014; Gatti et al., 2015; Piazzi et al., 2015, 2021; Cánovas-Molina et al., 2016; Ferrigno et al., 2017, 2018; Montefalcone et al., 2017; Sartoretto et al., 2017; Enrichetti et al., 2019).

FIGURE 1 | Location of the study area and the sampling sites. **(A)**
Bathymetric map of the study area, Marzamemi, Sicily, with the indication of
the ROV_290621_06 track (black line) and the sampling sites (CBR2_3_7c,
red dot and CBR2_4_21c, yellow dot). **(B)** Image from the
ROV_290621_06 in a setting similar to the sampling site CBR2_3_7c. **(C)**
Image from the ROV_290621_06 in a setting similar to the sampling site
CBR2_4_21c. Scale bars = 10 cm for both **(C)** and **(D)**.

One of the main goals of the project "CRESCIBLUREEF -
Grown in the blue: new technologies for knowledge and
conservation of Mediterranean reefs" (project FISR
2019_04543) is to understand the *tempo* and the mode of the
coralligenous inception and development, as well as the type of
accretionary structures and their growth rate, also in the
framework of the Holocene climate fluctuations.

Therefore, the appropriate identification of Coralligenous
represents a fundamental starting point for this purpose.
coralligenous build-ups indicated as pillars have already
been identified in the sea bottom off south Marzamemi
village (eastern Sicily, Ionian Sea, Italy) (Di Geronimo
et al., 2001, 2002). In this context, we collected two
coralligenous pillars at similar water depth but from
different settings in terms of build-up density. The aim of
this study is to identify and quantify the role of the different
builders, both from the surface and from the inner structures
by using photogrammetry and computed-tomography
technology. This knowledge appears fundamental to
properly addressing the efforts of monitoring, maintenance,
and restoration of such types of submarine habitats in the
long-term scenario, in the wider context of marine spatial
planning.

2 MATERIALS AND METHODS

We collected direct observations of the seafloor offshore
Marzamemi (**Figure 1A**) by using the ROV Steelhead
SEAMORE, property of the University of Milano-Bicocca,
during the first fieldwork survey of the CRESCIBLUREEF
project (20–30 June 2021). The ROV is equipped with low-
and high-quality cameras. Thanks to inspection
ROV_290621_06, we were able to identify the proper
sampling site, below the lower bathymetric limit of the
Posidonia oceanica meadow (**Figure 1A**).

Two coralligenous samples were collected by scuba divers
following the method of Bertolino et al. (2014) in the framework
of the second field campaign of the project (1–7 August 2021)
(**Figure 1A**). Samples have been marked with a spike on their
north side before the collection.

CBR2_3_7c (36°43.394′ N; 15°09.469′ E, **Figure 1A**) was
collected at a depth of 37 m, whereas CBR2_4_21c (36°43.454′
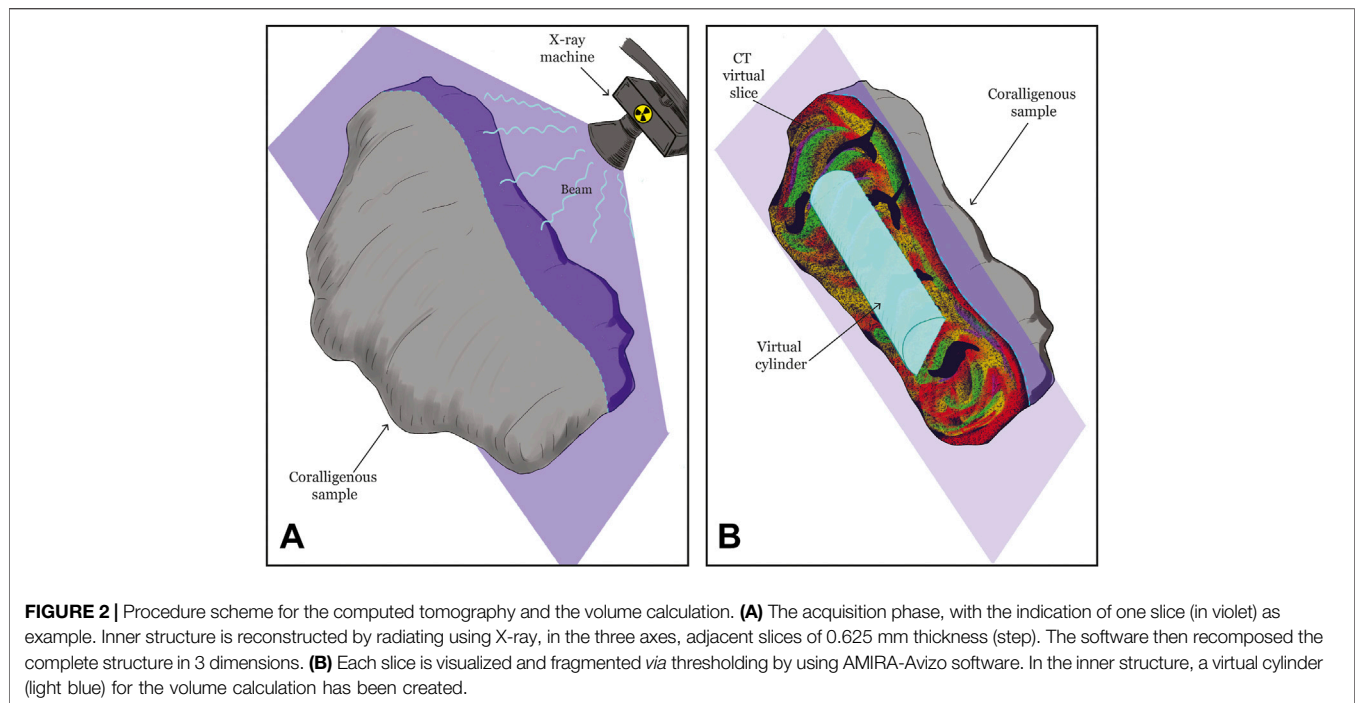N; 15°09.657′ E, **Figure 1A**) was collected at a depth of 36 m.

2.1 Photogrammetric Reconstruction
Images were acquired all around the two samples in their original
condition after recovery, to cover the entire surface with an
adequate overlap between adjacent pictures (70%–80%). After
the manual removal of the canopy with non-builder organisms,
samples have been pictured again with the same scheme to
produce a complete cover of the build-up.

All the images were processed using Agisoft Metashape®. This
software performs 3D reconstruction of objects from overlapping
images through a complete photogrammetric workflow (Anelli
et al., 2019; Olinger et al., 2019; Casoli et al., 2021). After the
alignment of the images, the obtained model has been scaled.
Then, a textured mesh was generated. From this 3D model, six
high-resolution scaled orthomosaics, representing all the sides of
the Coralligenous (north, east, west, south, top, and bottom),
were obtained and exported in TIFF format.

2.2 Object-Based Image Analysis and Classification of Orthomosaics
The analysis and classification of the orthomosaics obtained for each
side of Coralligenous were performed using eCognition Developer
9.5® (Trimble). This software allowed carrying out an object-based
image analysis (OBIA) to speed up the classification of the
orthomosaics and estimate the extensions of the different classes
(Blaschke, 2010; Fallati et al., 2020). As a first step, a multiresolution
segmentation algorithm, based on homogeneity criteria, was applied
to the orthomosaics. The image layer weights were set as identical for
the three RGB bands, and the optimal scale parameter found was
350. A shape value of 0.3 and compactness of 0.7 were established for
the homogeneity criteria. After the segmentation, a supervised
classification was applied, taking advantage of the features
calculated for each object such as the spectral value and size,
shape, texture, and proximity. Thanks to these parameters and
the high quality of orthomosaics, twelve classes were identified:
CCA + Peyssonneliales; CCA framework; soft algae; foraminifera;
sponges; cnidarians; mollusks (encrusting and boring); bryozoans;

FIGURE 2 | Procedure scheme for the computed tomography and the volume calculation. **(A)** The acquisition phase, with the indication of one slice (in violet) as example. Inner structure is reconstructed by radiating using X-ray, in the three axes, adjacent slices of 0.625 mm thickness (step). The software then recomposed the complete structure in 3 dimensions. **(B)** Each slice is visualized and fragmented *via* thresholding by using AMIRA-Avizo software. In the inner structure, a virtual cylinder (light blue) for the volume calculation has been created.

annelids (polychaetes); arthropods (barnacles); sediment; and cavities on the surface. CCA + Peyssonneliales includes living CCA and both completely calcified and fleshy Peyssonneliales, whereas the fleshy Peyssonneliales were missing after the canopy removal. The CCA framework includes dead CCA.

After the classification, the extension of each class, expressed in cm^2, was automatically calculated in eCognition and exported. Extension represents the cover as the surface occupied by a single class, not considering overgrowing.

Principal component analyses (PCAs) were conducted on the cover percentage values to define the differences between the two samples using the software PAST 4.04 (Hammer et al., 2001). The first PCA was conducted on the whole dataset; both on the original and after the removal of the canopy cover values. Two further PCAs were conducted considering the two samples separately.

2.3 Computed Tomography

For computed tomography (CT), we used the model Revolution EVO integrated with the scanner PET/TC Discovery MI - General Electric, property of "Fondazione Tecnomed" of the University of Milano-Bicocca based at the Nuclear Medicine Department in Monza, Italy.

The acquisition protocol used the following set parameters: 140 kV and step 0.625 mm. Each sample was scanned along the three main axes (**Figure 2A**). Images were reconstructed by using the axial filter "bone plus" to obtain the best possible visualization of carbonate fraction.

The results were analyzed using AMIRA-Avizo software by Thermo Fisher Scientific, whereby threshold images were generated in order to clearly delineate skeletal material from

empty space, as well as exclude sediment infilling. The results were visualized in three dimensions using the same software.

To compare the two Coralligenous in a more homogenous way, fragmentation *via* thresholding was quantified into two sub-volumes (two vertical cylinders, with a height of 30 and a diameter of 15 cm for CBR2_3_7c and a height of 22 and a diameter of 11 cm for CBR2_4_21c, **Figure 2B**). The difference in cylinder dimension is due to the real dimensions of coralligenous samples. Four density classes were identified using the multi-threshold tool: low-density (LD), medium-density (MD), high-density (HD), and ultrahigh-density (UHD). To validate the classes, we compared the identification with the samples. Void volume was measured and used to calculate the porosity of both samples, as the ratio between the total volume of the single cylinder and the total volume of its voids.

3 RESULTS

3.1 CBR2_3_7c

CBR2_3_7c was collected in an area characterized by high Coralligenous cover in the form of a hybrid bank (Bracchi et al., 2017), made of distinct coralligenous columns, sometimes coalescent, with a high cover of the seafloor (**Figure 1B**). Biogenic gravel occurs among coralligenous build-ups (**Figure 1B**). CBR2_3_7c is 56 cm high, with a circumference of 59 cm at the base, a circumference of 78 cm at the top and a maximum circumference of 116 cm (**Figure 3A**). The build-up was coalescent with a contiguous one, and therefore, it was broken not only at the base but also along its NE side. The weight of the sample is 35 kg.
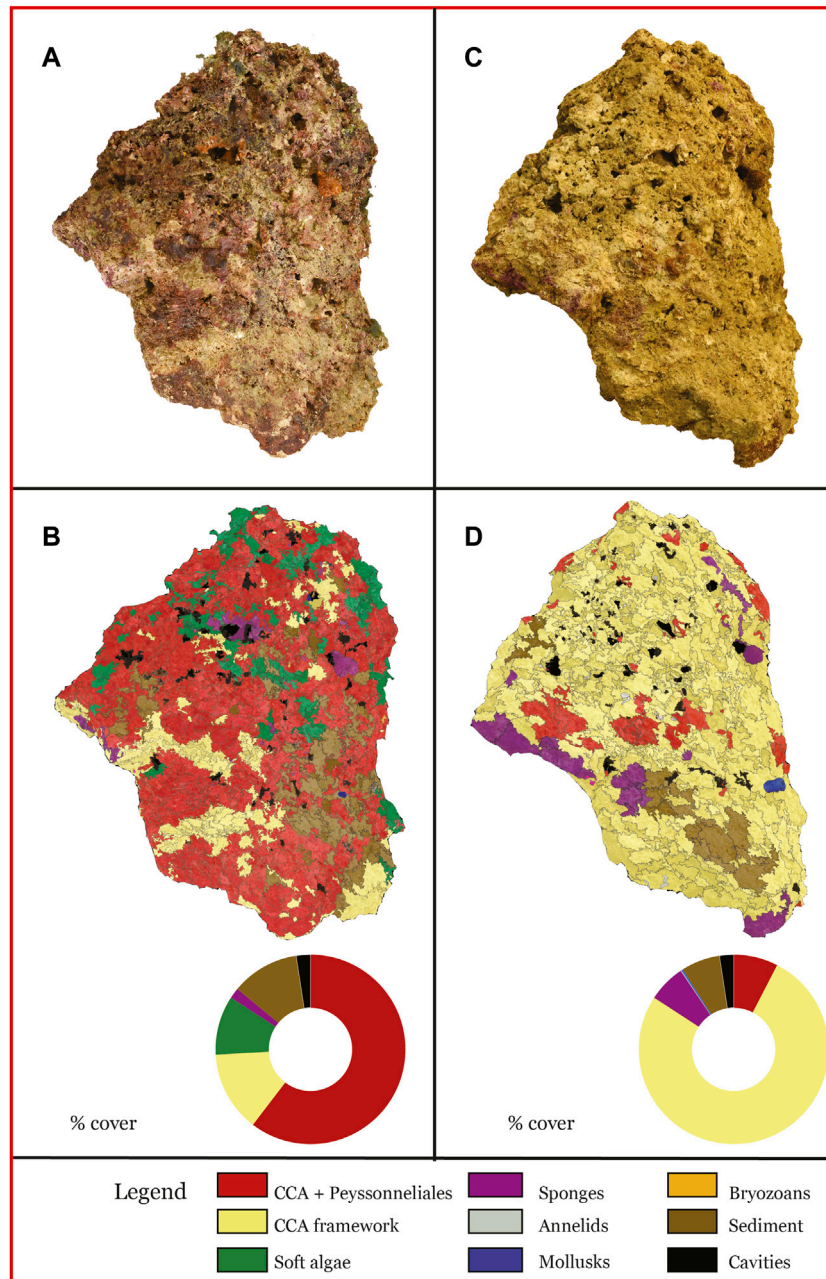
FIGURE 3 | East side of the sample CBR2_3_7c, pictured **(A,C)** and fragmented **(B,D)**. **(A)** Original east side; **(B)** results of the fragmentation of the east side with the ring chart of covers; **(C)** east side after the canopy removal; **(D)** results of the fragmentation of the east side after the canopy removal with the ring chart of covers. Among the 12 categories indicated in the Methods, only the ones actually detected have been reported in the legend.

3.1.1 Original Cover

The most abundant component is the CCA + Peyssonneliales class, with a cover ranging between 60.79% at the top and 38.69% at the bottom (**Figure 3A**; **Table 1**). Lateral cover ranges between 50.93% and 60.38% (**Figures 3A,B**, **4A**; **Table 1**). The CCA framework is the second component, with a cover ranging between 9.03% (south

side) and 50.35% (bottom side) (**Figure 4A**; **Table 1**). Soft algae are also abundant, up to 20.29% in the south side (**Figure 4A**; **Table 1**). All the animal groups have negligible covers, whereas sediment ranges between 3.85% (north side) and 13.41% (south side) (**Figure 4A**; **Table 1**). Cavities range between 0.93% (top side) and 2.42% (east side) (**Figures 3B**, **4A**; **Table 1**).

TABLE 1 | Cover of the identified classes on the surfaces of coralligenous samples CBR2_3_7c and CBR2_4_21c, at time of collection (O = original) and after the canopy removal (R). Results expressed in cover percentages.

		CBR2_3_7c						CBR2_4_21c					
		Top	North	East	South	West	Bottom	Top	North	East	South	West	Bottom
CCA +Peyssonneliales	O	60.79	57.80	60.38	52.86	50.93	38.69	46.24	59.36	30.41	54.06	49.56	18.12
	R	21.53	14.43	7.58	9.47	25.99	2.26	17.91	17.80	9.16	23.96	22.17	5.58
CCA framework	O	15.31	21.05	13.74	9.03	22.91	50.35	5.64	14.50	18.42	5.53	3.07	63.48
	R	63.98	71.73	76.57	79.38	57.85	76.47	56.54	64.59	74.61	64.51	51.06	85.66
Soft algae	O	15.27	14.24	10.07	20.29	10.44	1.44	17.50	14.39	31.60	24.09	28.01	5.94
	R	1.40	0.47	0.00	1.48	2.28	1.01	0.27	0.67	0.12	0.07	0.02	1.06
Foraminifers	O	0.03	0.00	0.01	0.00	0.00	0.00	0.02	0.02	0.01	0.00	0.00	0.04
	R	0.00	0.00	0.05	0.00	0.00	0.04	0.08	0.13	0.18	0.15	0.07	0.05
Sponges	O	1.30	1.74	1.80	3.14	2.92	1.79	1.17	4.42	0.72	0.00	0.85	0.25
	R	1.51	3.38	6.35	2.30	3.35	4.28	1.14	3.84	0.92	2.19	1.71	1.93
Annelids	O	0.06	0.08	0.00	0.00	0.01	0.84	0.10	0.55	0.85	0.00	0.05	2.25
	R	0.13	0.21	0.17	0.00	0.07	0.75	0.03	1.54	0.27	0.54	0.57	1.12
Cnidarians	O	0.00	0.00	0.00	0.00	0.00	0.00	0.00	0.07	0.00	0.00	0.00	0.00
	R	0.00	0.00	0.00	0.00	0.00	0.00	0.08	0.00	0.00	0.00	0.00	0.00
Mollusks	O	0.00	0.00	0.07	0.05	0.00	0.00	0.31	0.02	0.00	0.00	0.00	0.06
	R	0.00	0.02	0.28	0.33	0.00	0.03	0.39	0.00	0.00	0.00	0.00	0.02
Bryozoans	O	0.14	0.09	0.06	0.11	0.09	0.11	12.30	3.71	8.05	3.25	7.75	6.09
	R	0.10	0.43	0.03	0.15	1.09	0.46	0.26	2.10	3.93	0.37	0.78	1.21
Arthropods	O	0.00	0.00	0.00	0.00	0.00	0.00	0.01	0.03	0.00	0.04	0.00	0.00
	R	0.00	0.00	0.00	0.00	0.00	0.00	0.00	0.00	0.00	0.00	0.00	0.00
Sediment	O	6.16	3.85	11.45	13.41	11.11	4.66	16.07	2.58	9.20	12.60	10.08	3.41
	R	8.86	6.08	6.56	4.86	5.72	11.56	22.67	8.45	8.51	7.15	22.51	3.18
Cavities	O	0.93	1.14	2.42	1.10	1.59	2.11	0.64	0.35	0.74	0.44	0.62	0.36
	R	2.49	3.26	2.40	2.03	3.64	3.14	0.62	0.87	2.29	1.06	1.11	1.24

3.1.2 Cover After the Canopy Removal

The most abundant component is the CCA framework, with a cover ranging between 57.85% (west side) and 79.38% (south side) (**Figure 4A**; **Table 1**). The CCA + Peyssonneliales class is still important (cover range 2.26%–25.99%), together with sediment (cover range 4.86%–11.56%) (**Figure 4A**; **Table 1**). Soft algae are negligible as well as all the animal groups except for sponges, which range between 1.51 and 6.35% (**Figure 4A**; **Table 1**). Cavities range between 2.03% (south side) and 3.26% (north side) (**Figure 4A**; **Table 1**).

3.1.3 CT Fragmentation

A volume corresponding to the 58.38% of the biocostruction is composed of a dense framework (HD + UHD classes) (**Figure 5A**; **Table 2**). The low-density class accounts for 22.06%, whereas medium density accounts for 10.03% (**Figure 5A**; **Table 2**). Voids account for 28.40% (**Figure 5A**; **Table 2**). Calculated porosity is 0.28 (**Table 2**). The validation of the identified classes with the sample reveals that UHD, HD, and MD classes correspond to the CCA framework with different levels of lithification, whereas the LD class corresponds to cavities filled by non-lithified sediments.

3.2 CBR2_4_21c

The CBR2_4_21c sample was collected in the middle of a submarine channel consisting of biogenic gravel and sand where distinct, small, and sparse columns of Corralligenous characterize the seascape (**Figu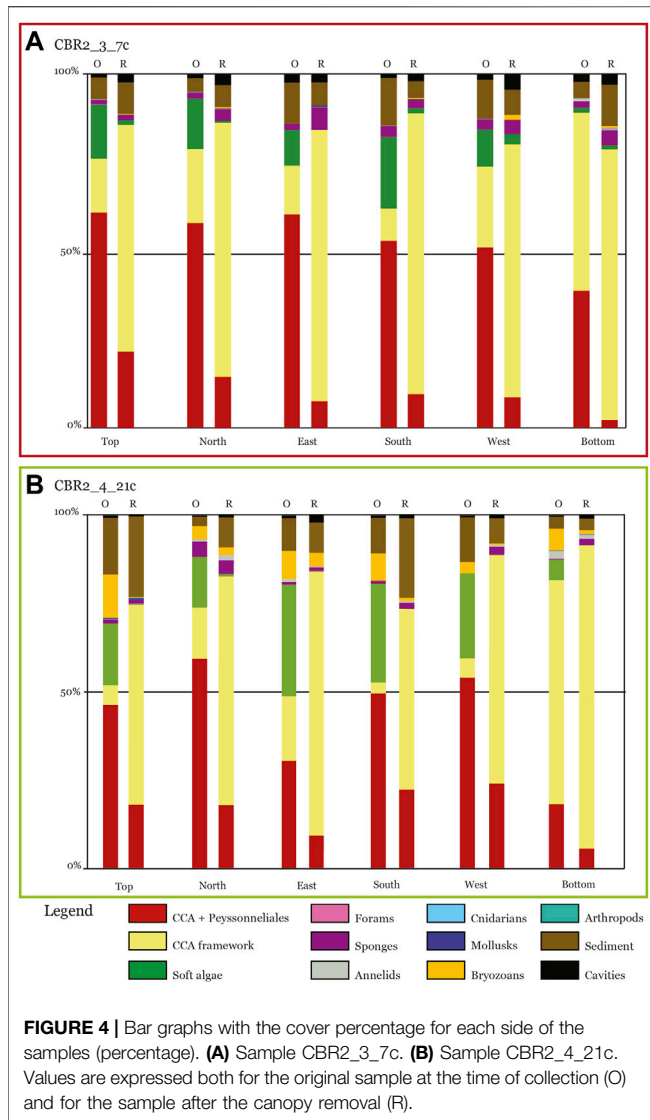re 1C**). CBR2_4_21c is 38 cm high, with a circumference of 71 cm at the base, a circumference of 52.5 cm at the top and a maximum circumference of 112 cm (**Figure 6**). The weight is 30 kg.

3.2.1 Original Cover

The most abundant component is the CCA + Peyssonneliales class, with a cover ranging between 18.12% (bottom side) and 59.36% (north side) (**Figures 4B**, **6B**; **Table 1**). Soft algae have important covers, ranging between 14.39% (north side) and 31.60% (east side), except for the bottom (5.94%) (**Figure 4B**; **Table 1**). The CCA framework is abundant only on the bottom side (63.48%), and it is relatively important in the north (14.50%) and east side (18.42%) (**Figures 4B**, **6B**; **Table 1**). All the animal groups are negligible except for the bryozoans (from 3.05% up to 12.30%). Sediment ranges between 2.58% (north side) and 16.07% (top side), whereas cavities are always less than 1% (**Figure 4B**; **Table 1**).

3.2.2 Cover After the Canopy Removal

The most abundant component is the CCA framework, with a cover ranging from 51.06% (west side) up to 85.66% (bottom side) (**Figure 4B**; **Table 1**). The CCA + Peyssonneliales class is still important (cover range 9.16%–23.96%), together with sediment (cover range 3.18%–22.67%) (**Figure 4B**; **Table 1**). All the animal groups are negligible, except for bryozoans and sponges, which range from 0.26% to 3.93% and from 0.92% and 3.84%, respectively (**Figure 4B**; **Table 1**). Sediment ranges between 3.18% (bottom side) and 22.67% (top side), whereas cavities range between 0.62% (top side) and 2.29% (east side) (**Figure 4B**; **Table 1**).

FIGURE 5 | Example of one slice per sample after the CT fragmentation *via* thresholding. **(A)** CBR2_3_7c fragmentation. **(B)** CBR2_4_21c f fragmentation. Light-blue lines indicate the sections of the cylindrical sub-volumes considered for the calculation.

FIGURE 4 | Bar graphs with the cover percentage for each side of the samples (percentage). **(A)** Sample CBR2_3_7c. **(B)** Sample CBR2_4_21c. Values are expressed both for the original sample at the time of collection (O) and for the sample after the canopy removal (R).

3.2.3 CT Fragmentation

The most abundant class in the framework of the sample CBR2-4_21c is represented by the medium-density (31.09%) followed by the high-density (23.04%) class (**Figure 5B**; **Table 2**). Voids account for 21.04% and calculated porosity is 0.21 (**Table 2**). The validation of the identified classes with the sample reveals that UHD, HD, and MD classes correspond to the CCA framework with different levels of lithification, whereas the LD class corresponds to cavities filled by still unlithified sediments.

3.3 PCA Analyses

PCAs easily distinguish between original samples and the same after the canopy removal (**Figure 7**). **Figure 7A** shows the PCA plot considering both samples and all sides, whereas **Figures 7B,C** present the same results considering CBR2_3_7c and CBR2_4_21c separately. Component 1, representing the CCA framework, easily distinguishes between original and "after the removal" samples (**Figure 7A**). This is the reason why all the
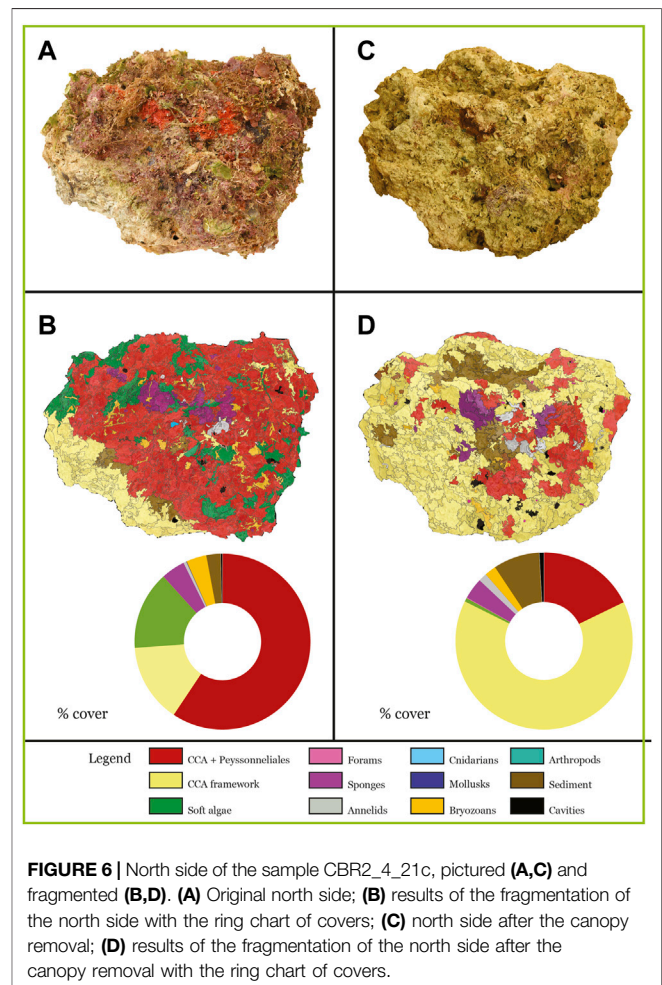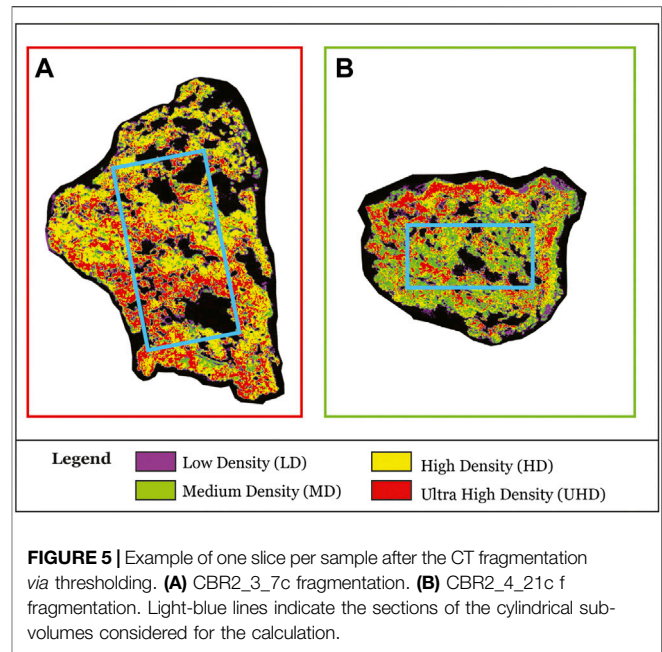

FIGURE 6 | North side of the sample CBR2_4_21c, pictured **(A,C)** and fragmented **(B,D)**. **(A)** Original north side; **(B)** results of the fragmentation of the north side with the ring chart of covers; **(C)** north side after the canopy removal; **(D)** results of the fragmentation of the north side after the canopy removal with the ring chart of covers.

TABLE 2 | Results of the fragmentation in density classes from the CT analysis. Volumes in mm^3 and percentage. LD, low-density; MD, medium-density; HD, high-density; UHD, ultrahigh-density.

		CBR2_3_7c	%	CBR2_4_21c	%
		mm^3		mm^3	
Volume	LD	535112	9.18	250512	9.42
	MD	584311	10.03	826887	31.09
	HD	1766900	30.32	612721	23.04
	UHD	1285660	22.06	399996	15.04
	Voids	1655197	28.40	569576	21.42
	Total volume	5827180		2659692	
	Porosity	0,28		0,21	

bottom sides are mixed (**Figure 7A**). Interestingly, in both CBR2_3_7c (**Figure 7B**) and CBR2_4_21c (**Figure 7C**), the two most different original surfaces are the north and south sides.

4 DISCUSSION

Several efforts have been made in the last decades to fill the gap in the knowledge of the so-called mesophotic biogenic reefs, also in the Mediterranean Sea. Coralligenous only partially overlaps with the wide range of the bioconstructions found in the mesophotic zone, developing at different depths and under different environmental factors (e.g., Cerrano et al., 2010, 2019; Bianchelli et al., 2013; Giusti et al., 2014; Cau et al., 2015; Grinyó et al., 2018).

Although the term coralligenous effectively identifies a heterogeneous bioconstruction (Pérès and Picard, 1964; Ballesteros, 2006; La Rivière et al., 2021), the use of this term for different types of bioherms and communities leads to possibly confusing different habitats/communities with each other, and consequently different mesophotic reefs, putting them all together under a unique definition.

Coralligenous samples examined in this study were collected below the bathymetric limit of the *Posidonia oceanica* meadow, as seen on the ROV (**Figures 1B,C**). The quantitative approach of this study confirms that the analyzed samples are dominated by CCA, in the form of living and dead CCA, and mineralized Peyssonneliales (**Figures 2**, **3**, **6**; **Table 1**), in agreement with the previous description of a coralligenous pillar in the area (Di Geronimo et al., 2002). We suggest that the CCA dominance, especially as primary substrate and in the inner structure, should identify the Coralligenous from all other different biogenic mesophotic reefs. This consideration finds a strong validation in the Quaternary fossil record, where analogous fossil reefs have been identified as Coralligenous, and they are mostly composed of CCA and lithified sediment, with a negligible contribution of all other components (Bosence and Pedley 1982; Carannante and Simone, 1996; Rasser, 2000; Nalin et al., 2006; Basso et al., 2007, 2009; Titschack et al., 2008; Bracchi et al., 2014, 2016, 2019). We consequently interpret our samples as true examples of Coralligenous circalittoral biocoenosis as originally defined by Pérès and Picard (1964). As supported by the results of PCA analyses (**Figure 7**), the different cover values clearly distinguish the original samples from those after the canopy removal

(**Figures 2**, **5**; **Table 1**), showing that the surface often shows a high biodiversity because the solid substrate supports a wide range of communities. Nevertheless, we demonstrated that CCA are also abundant at the surface. Therefore, the appropriate identification of this class in visual methods, although applied only at surfaces, should be considered for the identification of the Coralligenous, when possible.

The CT revealed that the CCA framework, corresponding to classes from MD up to UHD, dominates the inner structure, although with different densities (**Figure 5**; **Table 2**). The framework represents a combination of algal thalli together with sediment that can fill the empty space among CCA crusts or inner voids. CCA surely represent the basic framework for the tridimensional development of the build-up, but also the role of sediment and lithification is crucial for its development. Two types of micrite are possibly present: detrital micrite and autochthonous micrite. The first type derives from physical processes, notably erosion, transport, and deposition. The lithification rate of this type of micrite is generally low and may take place over time after the primary framework is formed. The second type could derive from induced biomineralization, mediated by microbial metabolic activities, or influenced biomineralization, mediated by organic matter decay (Perry et al., 2007; Altermann et al., 2009; Dupraz et al., 2009; Anbu et al., 2016; Guido et al., 2019; Görgen et al., 2020; Riding and Virgone, 2020). The occurrence of autochthonous micrite allows hypothesizing a possible contribution of a non-skeletal carbonate component in the strengthening of the primary framework due to the sin-depositional cementation of this micrite type. Further specific micromorphological and biogeochemical analyses will allow elucidating the detrital *vs.* autochthonous origin of the micrite sediments and clarifying the role of the different types of micrites in terms of coralligenous density parameters.

The Coralligenous typically presents a cavernous structure (Ballesteros, 2006), and the occurrence of cavities and crevices at different scales contributes to the creation of several ecological niches that in turn enhance its values in term of biodiversity (Bertolino et al., 2013, 2017a; b; 2019, Costa et al., 2019). In our samples occur several surficial and internal cavities sometimes not in contact with the surface as inner voids. Interestingly, the surface shows few visible centimeter cavities (**Table 1**), whereas the CT shows a very porous framework, with centimetric voids (**Figure 5**).

FIGURE 7 | Principal component analyses (PCAs) of the percentage cover of the coralligenous side, showing the scatter plot with the Component 1 and 2 axes. **(A)** PCA of all the sides, both original (O) and after the canopy removal (R); **(B)** only CBR2_3_7c; **(C)** only CBR2_4_21c.
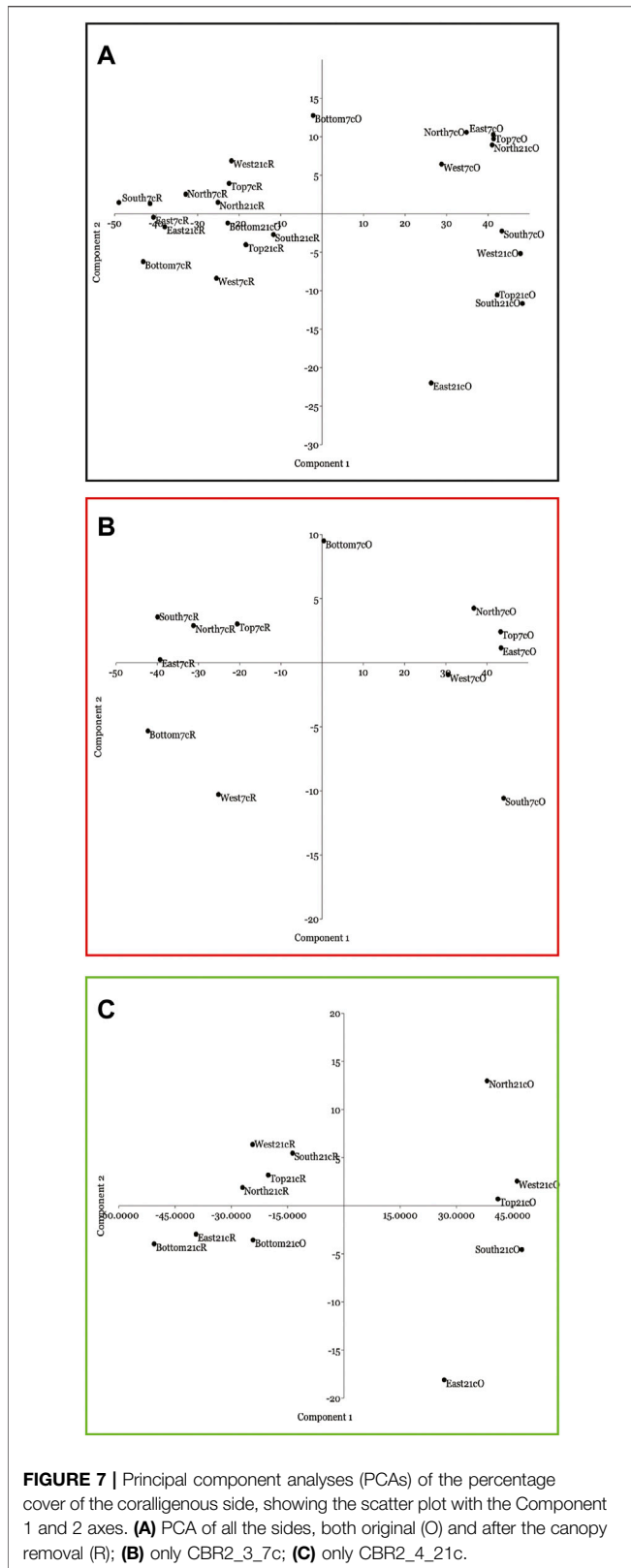
CT shows that CBR2_3_7c has a more compact inner structure, and voids are generally coarser than CBR2_4_21c (**Figure 5A**; **Table 2**).

CBR2_4_21c is dominated by the MD to HD classes, actually showing a generally much more open framework with algal thalli separated by empty spaces, only sometimes filled by loose sediment, and generally fewer and smaller voids (**Figure 5B**; **Table 2**). The calculated porosity corresponds to 0.28 (CBR2_3_7c) and 0.21 (CBR2_4_21c) and these represent the first quantitative data about coralligenous porosity. The reported values suggest that a more compact material characterizes CBR2_3_7c with respect to CBR2_4_21c, despite the bigger inner voids. This variability can be related to the different density of Coralligenous at the habitat scale (**Figures 1B,C**). CBR2_4_21c developed in the middle of a submarine channel where transport of currents and sediments can generate much more turbidity with respect to CBR2_3_7c, which is instead more protected from sedimentation by its surroundings. This is also reflected in the cover percentage values, where the maximum sediment cover is observed on the top side of CBR2_4_21c (22.7%, **Table 1**). Further study will deeply investigate these aspects.

CCA in the Coralligenous have a growth rate ranging between 0.006 and 0.83 mm/yr (Ingrosso et al., 2018). Di Geronimo et al. (2002) specifically indicated 0.27 mm/year for samples collected in the same area. This extremely slow development is compatible with the scale of geological time, which is the appropriate scale of observation of the genetic process at the base of the persistent substrate of biogenic origin. Efforts in conservation and management should therefore consider this specific substrate for ensuring a proper management of the coralligenous habitat.

Multiscale remote and direct visual methods (pros and cons) applied to Coralligenous have been summarized in the study by Zapata-Ramírez et al. (2013). In our work, we applied both 2D (OBIA classification) and 3D (CT) techniques to quantitatively define the contribution of organisms, and among them, of the builders, in the Coralligenous at the scale of singular build-up with solid results. However, the orthomosaic fragmentation of the sample sides and subsequent OBIA classification present some limits like 1) the minimum dimension of the fragmentation setting and 2) the maximum resolution of the orthomosaic image. This translates in some limitations in the detection of some components of the fragmentation, if too small. Despite this apparent limitation, we were still able to depict high biodiversity at the surface and the contribution of all taxa, albeit with various degrees, to the surface cover (**Table 1**). These results confirm that coralligenous represents a hotspot of biodiversity, hosting highly diversified flora and fauna at its surface (**Figures 4, 7**; **Table 1**) and that this technique is still appropriate. In addition, we were able to detect a good variability within the two samples and among sides of the same sample (**Figures 3, 4, 6, 7**; **Table 1**), which suggests caution when comparing visual census observations from different sites for ecological status assessment and monitoring purposes.

CCA often serve as substrate for many different encrusting components, which means that the real CCA cover can be partially underestimated because CCA are not visible at the surface. Moreover, mineralized and unmineralized Peyssonneliales were not automatically distinguishable *via* fragmentation and OBIA classification. After the canopy

removal, the cover of the class CCA + Peyssonneliales no longer includes unmineralized Peyssonneliales. The comparison of the values of this class before and after the canopy removal is indicative of the contribution of unmineralized Peyssonneliales. As observed in **Table 1**, the values of this class before and after the canopy removal strongly decrease, suggesting that unmineralized Peyssonneliales are abundant and contribute to hiding the CCA on the bioconstruction surface. The risk of underestimating the CCA contributing to Coralligenous by surface observation is therefore an evident limit, and also, this aspect should be correctly considered for an adequate definition of Coralligenous.

5 CONCLUSION

The fine scale analysis of two discrete coralligenous build-ups collected offshore Marzamemi (Sicily, Ionian Sea) allowed univocally and quantitatively defining the role of different reef-builders in this type of Mediterranean bioconstruction. CCA dominate the surface of the structures, both in the original condition and after the removal of the canopy of fleshy and unmineralized organisms. Their skeletons, densely packed together with lithified sediments, form the primary framework of the bioconstruction attributing them a medium- to ultrahigh-density. Porosity in Coralligenous has been assessed as 0.21 and 0.28 for the first time. The present study approach enables us to confirm that the Marzamemi Coralligenous is a primary biogenic hard substrate dominated by CCA, which play a fundamental role as physical and permanent builders compared to all other taxonomic groups that provide negligible contributions. The long-time development of this primary substrate also supports important communities of high biodiversity value on its surface and into its crevices that, however, represent non-builder components.

Although Coralligenous shows a high heterogeneity, this term has been apparently applied to circalittoral mesophotic reefs different in respect to the original definition. Instead, the genetic nature of this specific substrate should be considered in order to develop appropriate measures for management and conservation to guarantee a future for this specific type of habitat.

DATA AVAILABILITY STATEMENT

The original contributions presented in the study are included in the article/Supplementary Material; further inquiries can be directed to the corresponding author.

AUTHOR CONTRIBUTIONS

Conceptualization: VB, AR, and DB; methodology: VB, PB, LF, RL, MN, and EP; formal analysis: VB, PB, and LF; investigation: VB, PB, LF, AV, AS, AR, RS, RL, and DB; data curation: VB, PB, and LF; writing—original draft preparation: VB and LF; writing—review and editing: VB, PB, LF, AV, AS, AR, RS, AG, MB, GC, and DB; supervision: DB and AR; project administration: DB, AR, and MM; funding acquisition: DB, AR, and MM. All authors have read and agreed to the published version of the manuscript.

REFERENCES

Altermann, W., Böhmer, C., Gitter, F., Heimann, F., Heller, I., Läuchli, B., et al. (2009). Defining biominerals and organominerals: Direct and indirect indicators of life. Perry et al., Sedimentary Geology, 201, 157-179. *Sediment. Geol.* 213 (3-4), 150–151. doi:10.1016/j.sedgeo.2008.04.001

Anbu, P., Kang, C.-H., Shin, Y.-J., and So, J.-S. (2016). Formations of Calcium Carbonate Minerals by Bacteria and its Multiple Applications. *SpringerPlus* 5, 250. doi:10.1186/s40064-016-1869-2

Anelli, M., Julitta, T., Fallati, L., Galli, P., Rossini, M., and Colombo, R. (2019). Towards New Applications of Underwater Photogrammetry for Investigating Coral Reef Morphology and Habitat Complexity in the Myeik Archipelago, Myanmar. *Geocarto Int.* 34 (5), 459–472. doi:10.1080/10106049.2017.1408703

Ballesteros, E. (2006). "Mediterranean Coralligenous Assemblages," in *Oceanogr. Mar. Biol. Ann. Rev.* Editor H. Barners (London, EN: LTD Press), 123–195. doi:10.1201/9781420006391.ch4

Basso, D., Nalin, R., and Massari, F. (2007). Genesis and composition of the Pleistocene Coralligene de plateau of the Cutro Terrace (Calabria, southern Italy). *njgpa* 244 (2), 173–182. doi:10.1127/0077-7749/2007/0244-0173

Basso, D., Nalin, R., and Nelson, C. S. (2009). Shallow-water *Sporolithon* Rhodoliths from North Island (New Zealand). *Palaios* 24, 92–103. doi:10.2110/palo.2008.p08-048r

Bellan-Santini, D., Lacaze, J. C., and Poizat, C. (1994). *Les biocénoses marines et littorales de Méditerranée, Synthèse, menaces et perspectives*. Collect. Patrim. Nat., Paris: Muséum National d'Histoire Naturelle, Sécretariat de la Flore et de la Faune.

Bertolino, M., Cerrano, C., Bavestrello, G., Carella, M., Pansini, M., and Calcinai, B. (2013). Diversity of Porifera in the Mediterranean Coralligenous Accretions, with Description of a New Species. *Zookeys* 336, 1–37. doi:10.3897/zookeys.336.5139

Bertolino, M., Calcinai, B., Cattaneo-Vietti, R., Cerrano, C., Lafratta, C., Pansini, M., et al. (2014). Stability of the Sponge Assemblage of Mediterranean Coralligenous Concretions Along a Millennial Time Span. *Mar. Ecol.* 35, 149–158. doi:10.1111/maec.12063

Bertolino, M., Cattaneo-Vietti, R., Costa, G., Pansini, M., Fraschetti, S., and Bavestrello, G. (2017a). Have Climate Changes Driven the Diversity of a Mediterranean

Coralligenous Sponge Assemblage on a Millennial Timescale? *Palaeogeogr. Palaeoclimatol. Palaeoecol.* 487, 355–363. doi:10.1016/j.palaeo.2017.09.020

Bertolino, M., Costa, G., Carella, M., Cattaneo-Vietti, R., Cerrano, C., Pansini, M., et al. (2017b). The Dynamics of a Mediterranean Coralligenous Sponge Assemblage at Decennial and Millennial Temporal Scales. *PloS One* 12 (5), e0177945. doi:10.1371/journal.pone.0177945

Bertolino, M., Costa, G., Cattaneo-Vietti, R., Pansini, M., Quarta, G., Calcagnile, L., et al. (2019). Ancient and Recent Sponge Assemblages from the Tyrrhenian Coralligenous over Millennia (Mediterranean Sea). *Facies* 65 (3), 1–12. doi:10.1007/s10347-019-0573-4

Bianchelli, S., Pusceddu, A., Canese, S., Greco, S., and Danovaro, R. (2013). High Meiofaunal and Nematodes Diversity Around Mesophotic Coral Oases in the Mediterranean Sea. *PLoS One* 8, e66553. doi:10.1371/journal.pone.0066553

Blaschke, T. (2010). Object Based Image Analysis for Remote Sensing. *ISPRS J. Photogrammetry Remote Sens.* 65 (1), 2–16. doi:10.1016/j.isprsjprs.2009.06.004

Bosence, D. W. J., and Pedley, H. M. (1982). Sedimentology and Palaeoecology of a Miocene Coralline Algal Biostrome from the Maltese Islands. *Palaeogeogr. Palaeoclimatol. Palaeoecol.* 38, 9–43. doi:10.1016/0031-0182(82)90062-1

Bracchi, V. A., Basso, D., Marchese, F., Corselli, C., and Savini, A. (2017). Coralligenous Morphotypes on Subhorizontal Substrate: A New Categorization. *Cont. Shelf Res.* 144, 10–20. doi:10.1016/j.csr.2017.06.005

Bracchi, V. A., Basso, D., Savini, A., and Corselli, C. (2019). Algal Reefs (Coralligenous) from Glacial Stages: Origin and Nature of a Submerged Tabular Relief (Hyblean Plateau, Italy). *Mar. Geol.* 411, 119–132. doi:10.1016/j.margeo.2019.02.008

Bracchi, V. A., Nalin, R., and Basso, D. (2014). Paleoecology and Dynamics of Coralline Dominated Facies during a Pleistocene Transgressive-Regressive Cycle (Capo Colonna Marine Terrace, Southern Italy). *Palaeogeogr. Palaeoclimatol. Palaeoecol.* 414, 296–309. doi:10.1016/j.palaeo.2014.09.016

Bracchi, V. A., Nalin, R., and Basso, D. (2016). Morpho-structural Heterogeneity of Shallow-Water Coralligenous in a Pleistocene Marine Terrace (Le Castella, Italy). *Palaeogeogr. Palaeoclimatol. Palaeoecol.* 454, 101–112. doi:10.1016/j.palaeo.2016.04.014

Bracchi, V., Savini, A., Marchese, F., Palamara, S., Basso, D., and Corselli, C. (2015). Coralligenous Habitat in the Mediterranean Sea: a Geomorphological Description from Remote. *Ijg* 134, 32–40. doi:10.3301/IJG.2014.16

Cánovas-Molina, A., Montefalcone, M., Vassallo, P., Morri, C., Bianchi, C. N., and Bavestrello, G. (2016). Combining Literature Review, Acoustic Mapping and *In Situ* Observations: an Overview of Coralligenous Assemblages in Liguria (NW Mediterranean Sea). *Sci. Mar.* 80, 7–16. doi:10.3989/scimar.04235.23a

Carannante, G., and Simone, L. (1996). "Rhodolith Facies in the Central-southern Apennines Mountains, Italy," in *Models for Carbonate Stratigraphy from Miocene Reef Complexes of Mediterranean Regions*. Editors E. K. Franseen, M. Esteban, W. C. Ward, and J. M. Rouchy (Italy: SEPM Concepts in Sedimentology and Palaeontology), 5, 261–275. doi:10.2110/csp.96.01.0261

Casoli, E., Ventura, D., Mancini, G., Pace, D. S., Belluscio, A., and Ardizzone, G. (2021). High Spatial Resolution Photo Mosaicking for the Monitoring of Coralligenous Reefs. *Coral Reefs* 40 (4), 1267–1280. doi:10.1007/s00338-021-02136-4

Cau, A., Follesa, M. C., Moccia, D., Alvito, A., Bo, M., Angiolillo, M., et al. (2015). Deepwater corals biodiversity along roche du large ecosystems with different habitat complexity along the south Sardinia continental margin (CW Mediterranean Sea). *Mar. Biol.* 162, 1865–1878. doi:10.1007/s00227-015-2718-5

Cecchi, E., Gennaro, P., Piazzi, L., Ricevuto, E., and Serena, F. (2014). Development of a New Biotic Index for Ecological Status Assessment of Italian Coastal Waters Based on Coralligenous Macroalgal Assemblages. *Eur. J. Phycol.* 49, 298–312. doi:10.1080/09670262.2014.918657

Cerrano, C., Bastari, A., Calcinai, B., Di Camillo, C., Pica, D., Puce, S., et al. (2019). Temperate Mesophotic Ecosystems: Gaps and Perspectives of an Emerging Conservation Challenge for the Mediterranean Sea. *Eur. Zoological J.* 86 (1), 370–388. doi:10.1080/24750263.2019.1677790

Cerrano, C., Bavestrello, G., Bianchi, C. N., Calcinai, B., Cattaneo-Vietti, R., Morri, C., et al. (2001). "The Role of Sponge Bioerosion in Mediterranean Coralligenous Accretion," in *Mediterranean Ecosystems*. Editors F. M. Faranda, L. Guglielmo, and G. Spezie (Milano: Springer), 235–240. doi:10.1007/978-88-470-2105-1_30

Cerrano, C., Danovaro, R., Gambi, C., Pusceddu, A., Riva, A., and Schiaparelli, S. (2010). Gold Coral (*Savalia savaglia*) and Gorgonian Forests Enhance Benthic Biodiversity and Ecosystem Functioning in the Mesophotic Zone. *Biodivers. Conserv.* 19, 153–167. doi:10.1007/s10531-009-9712-5

Chimienti, G., De Padova, D., Mossa, M., and Mastrototaro, F. (2020). A Mesophotic Black Coral Forest in the Adriatic Sea. *Sci. Rep.* 10, 8504. doi:10.1038/s41598-020-65266-9

Corriero, G., Pierri, C., Mercurio, M., Nonnis Marzano, C., Onen Tarantini, S., Gravina, M. F., et al. (2019). A Mediterranean Mesophotic Coral Reef Built by Non-symbiotic Scleractinians. *Sci. Rep.* 9, 3601. doi:10.1038/s41598-019-40284-4

Costa, G., Bavestrello, G., Micaroni, V., Pansini, M., Strano, F., and Bertolino, M. (2019). Sponge Community Variation along the Apulian Coasts (Otranto Strait) over a Pluri-Decennial Time Span. Does Water Warming Drive a Sponge Diversity Increasing in the Mediterranean Sea? *J. Mar. Biol. Ass.* 99 (7), 1519–1534. doi:10.1017/s0025315419000651

Deter, J., Descamp, P., Ballesta, L., Boissery, P., and Holon, F. (2012). A Preliminary Study toward an Index Based on Coralligenous Assemblages for the Ecological Status Assessment of Mediterranean French Coastal Waters. *Ecol. Indic.* 20, 345–352. doi:10.1016/j.ecolind.2012.03.001

Di Geronimo, I., Di Geronimo, R., Improta, S., Rosso, A., and Sanfilippo, R. (2001). Preliminary Observations on a Columnar Coralline Build-Up from off SE Sicily in Proceedings of the Conference of the Society o Marine Biology, Sharm El Sheikh, May 13–20 2000. *Biol. Mar. Medit.* 8 (1), 1–10.

Di Geronimo, I., Di Geronimo, R., Rosso, A., and Sanfilippo, R. (2002). Structural and Taphonomic Analysis of a Columnar Coralline Algal Build-Up from SE Sicily. *Geobios* 35, 86–95. doi:10.1016/S0016-6995(02)00050-5

Dupraz, C., Reid, R. P., Braissant, O., Decho, A. W., Norman, R. S., and Visscher, P. T. (2009). Processes of Carbonate Precipitation in Modern Microbial Mats. *Earth-Science Rev.* 96, 141–162. doi:10.1016/j.earscirev.2008.10.005

Enrichetti, F., Bava, S., Bavestrello, G., Betti, F., Lanteri, L., and Bo, M. (2019). Artisanal Fishing Impact on Deep Coralligenous Animal Forests: A Mediterranean Case Study of Marine Vulnerability. *Ocean Coast. Manag.* 177, 112–126. doi:10.1016/J.OCECOAMAN.2019.04.021

Fagerström, J. A. (1991). Reef-building Guilds and a Checklist for Determining Guild Membership. *Coral Reefs* 10, 47–52. doi:10.1007/BF00301908

Fallati, L., Saponari, L., Savini, A., Marchese, F., Corselli, C., and Galli, P. (2020). Multi-temporal UAV Data and Object-Based Image Analysis (OBIA) for Estimation of Substrate Changes in a Post-bleaching Scenario on a Maldivian Reef. *Remote Sens.* 12 (13), 2093. doi:10.3390/rs12132093

Feldmann, J. (1937). *Recherches sur la Végétation Marine de la Méditerranée: la Côte des Albères*. Paris: Rouen: Wolf.

Ferrigno, F., Russo, G. F., and Sandulli, R. (2017). Coralligenous Bioconstructions Quality Index (CBQI): a Synthetic Indicator to Assess the Status of Different Types of Coralligenous Habitats. *Ecol. Indic.* 82, 271–279. doi:10.1016/j.ecolind.2017.07.020

Ferrigno, F., Russo, G. F., Semprucci, F., and Sandulli, R. (2018). Unveiling the State of Some Underexplored Deep Coralligenous Banks in the Gulf of Naples (Mediterranean Sea, Italy). *Regional Stud. Mar. Sci.* 22, 82–92. doi:10.1016/j.rsma.2018.05.006

Gatti, G., Bianchi, C. N., Morri, C., Montefalcone, M., and Sartoretto, S. (2015). Coralligenous Reefs State along Anthropized Coasts: Application and Validation of the COARSE Index, Based on a Rapid Visual Assessment (RVA) Approach. *Ecol. Indic.* 52, 567–576. doi:10.1016/j.ecolind.2014.12.026

Giusti, M., Innocenti, C., and Canese, S. (2014). Predicting Suitable Habitat for the Gold Coral *Savalia savaglia* (Bertoloni, 1819) (Cnidaria, Zoantharia) in the South Tyrrhenian Sea. *Cont. Shelf Res.* 81, 19–28. doi:10.1016/j.csr.2014.03.011

Görgen, S., Benzerara, K., Skouri-Panet, F., Gugger, M., Chauvat, F., and Cassier-Chauvat, C. (2020). The Diversity of Molecular Mechanisms of Carbonate Biomineralization by Bacteria. *Discov. Mat.* 1, 2. doi:10.1007/s43939-020-00001-9

Grinyó, J., Viladrich, N., Díaz, D., Muñoz, A., Mallol, S., Salazar, J., et al. (2018). Reproduction, Energy Storage and Metabolic Requirements in a Mesophotic Population of the Gorgonian Paramuricea Macrospina. *PLoS One* 13, e0203308. doi:10.1371/journal.pone.0203308

Guido, A., Gerovasileiou, V., Russo, F., Rosso, A., Sanfilippo, R., Voultsiadou, E., et al. (2019). Composition and Biostratinomy of Sponge-Rich Biogenic Crusts

in Submarine Caves (Aegean Sea, Eastern Mediterranean). *Palaeogeogr. Palaeoclimatol. Palaeoecol.* 534, 109338. doi:10.1016/j.palaeo.2019.109338

Hammer, Ø., Harper, D. A. T., and Ryan, P. D. (2001). Past: Paleontological Statistics Software Package for Education and Data Analysis. *Palaeontol. Electron.* 4 (4), 1–9.

Hong, J. S. (1982). Contribution a l'étude des Peuplements d'un Fond de Concrétionnement Corllaigène dans la Région Marsaillaise en Méditerénée Nord-Occidentale. *Bull. Korea Oc. Res. Develop. Inst.* 4, 27–51.

Ingrosso, G., Abbiati, M., Badalamenti, F., Bavestrello, G., Belmonte, G., Cannas, R., et al. (2018). Mediterranean Bioconstructions along the Italian Coast. *Adv. Mar. Biol.* 79, 61–136. doi:10.1016/bs.amb.2018.05.001

Kipson, S., Fourt, M., Teixidó, N., Cebrian, E., Casas, E., Ballesteros, E., et al. (2011). Rapid Biodiversity Assessment and Monitoring Method for Highly Diverse Benthic Communities: A Case Study of Mediterranean Coralligenous Outcrops. *PLoS ONE* 6 (11), e27103. doi:10.1371/journal.pone.0027103

La Rivière, M., Michez, N., Delavenne, J., Andres, S., Fréjefond, C., Janson, A-L., et al. (2021). *Fiches descriptives des biocénoses benthiques de Méditerranée*. Paris: UMS PatriNat (OFB-CNRS-MNHN), 660.

Laborel, J. (1961). Le concrétionnement algal "Coralligene" et son importance géomorphologique en Méditerranée. *Rec. Trav. Stn. Mar. d'Endoume* 37 (27), 37–60.

Laubier, L. (1966). Le coralligène des Albères: monographie biocénotique. *Ann. l'Institut Océanogr. Monaco* 43, 139–316.

Littler, M. M. (1972). "The Crustose Corallinaceae," in *Oceanography and Marine Biology: An Annual Review*. Editor H. Barners (London, EN: LTD Press), 311–347.

Marchese, F., Bracchi, V. A., Lisi, G., Basso, D., Corselli, C., and Savini, A. (2020). Assessing Fine-Scale Distribution and Volume of Mediterranean Algal Reefs through Terrain Analysis of Multibeam Bathymetric Data. A Case Study in the Southern Adriatic Continental Shelf. *Water* 12, 157. doi:10.3390/w12010157

Marion, A. F. (1883). Esquisse d'une topographie zoologique du Golfe de Marseille. *Ann. Mus. Hist. Natur. Marseille* 1, 1–108.

Montefalcone, M., Morri, C., Bianchi, C. N., Bavestrello, G., and Piazzi, L. (2017). The Two Facets of Species Sensitivity: Stress and Disturbance on Coralligenous Assemblages in Space and Time. *Mar. Pollut. Bull.* 117, 229–238. doi:10.1016/j.marpolbul.2017.01.072

MSFD, EC (2008). *Directive 2008/56/EC of the European Parliament and of the Council of 17 June 2008 Establishing a Framework for Community Action in the Field of Marine Environmental Policy (Marine Strategy Framework Directive, Bruxelles)*.

Musard, O., Le Dû-Blayo, L., Francour, P., Beurier, J. P., Feunteun, E., and Talassinos, L. (2014). *Underwater Seascapes. From Geographical to Ecological Perspectives*. Berlin: Springer International Publishing.

Nalin, R., Basso, D., and Massari, F. (2006). Pleistocene coralline algal build-ups (coralligène de plateau) and associated bioclastic deposits in the sedimentary cover of Cutro marine terrace (Calabria, southern Italy). *Geol. Soc. Lond. Spec. Publ.* 255, 11–22. Cool-Water Carbonates: Depositional Systems and Palaeoenvironmental Controls, Editors H.M. Pedley, G. Carannante (London: The Geological Society of London). doi:10.1144/GSL.SP.2006.255.01.02

Olinger, L. K., Scott, A. R., McMurray, S. E., and Pawlik, J. R. (2019). Growth Estimates of Caribbean Reef Sponges on a Shipwreck Using 3D Photogrammetry. *Sci. Rep.* 9 (1), 1–12. doi:10.1038/s41598-019-54681-2

Pérès, J. M. (1982). "Major Benthic Assemblages," in *Marine Ecology*. Editor O. Kinne (London: John-Wiley Publ.), 5, 373–522.

Pérès, J. M., and Picard, J. (1964). Nouveau manuel de bionomie benthique de la Méditerranée. *Rec. Trav. Stat. Mar. Endoume* 31 (47), 1–37.

Perry, R. S., Mcloughlin, N., Lynne, B. Y., Sephton, M. A., Oliver, J. D., Perry, C. C., et al. (2007). Defining Biominerals and Organominerals: Direct and Indirect Indicators of Life. *Sediment. Geol.* 201, 157–179. doi:10.1016/j.sedgeo.2007.05.014

Piazzi, L., Gennaro, P., Cecchi, E., Bianchi, C. N., Cinti, M. F., Gatti, G., et al. (2021). Ecological Status of Coralligenous Assemblages: Ten Years of Application of the ESCA Index from Local to Wide Scale Validation. *Ecol. Indic.* 121, 107077. doi:10.1016/j.ecolind.2020.107077

Piazzi, L., Gennaro, P., Cecchi, E., and Serena, F. (2015). Improvement of the ESCA Index for the Evaluation of Ecological Quality of Coralligenous Habitat under the European Framework Directives. *Medit. Mar. Sci.* 16, 419–426. doi:10.12681/mms.1029

Ponti, M., Turicchia, E., Ferro, F., Cerrano, C., and Abbiati, M. (2018). The Understorey of Gorgonian Forests in Mesophotic Temperate Reefs. *Aquat. Conserv. Mar. Freshw. Ecosyst.* 28, 1153–1166. doi:10.1002/aqc.2928

Pruvot, G. (1895). Coup d'oeil sur la distribution générale des invertébrés dans la région de Banyuls (Golfe du Lion). *Arch. Zool. Exp. Gén.* 3, 629–658.

Pruvot, G. (1894). Sur les fonds sous-marins de la région de Banyuls et du cap de Creus. *Comp. Rend. Acad. Sci.* 118, 203–206.

Rasser, M. W. (2000). Coralline Red Algal Limestones of the Late Eocene Alpine Foreland Basin in Upper Austria: Component Analysis, Facies and Palecology. *Facies* 42 (1), 59–92. doi:10.1007/BF02562567

Riding, R. (2002). Structure and Composition of Organic Reefs and Carbonate Mud Mounds: Concepts and Categories. *Earth-Science Rev.* 58, 163–231. doi:10.1016/S0012-8252(01)00089-7

Riding, R., and Virgone, A. (2020). Hybrid Carbonates: *In Situ* Abiotic, Microbial and Skeletal Co-precipitates. *Earth-Science Rev.* 208, 103300. doi:10.1016/j.earscirev.2020.103300

Risso, A. (1826). "Histoire Naturelle des Principales Productions de l'Europe Méridionale et Particulièrement de Celles des Environs de Nice et des Alpes Maritimes,". Editor V. F.-G. Tome (Levrault, Paris), 400 pp.

Rosso, A., and Sanfilippo, R. (2009). "The Contribution of Bryozoans and Serpuloideans to Coralligenous Concretions From SE Sicily," in UNEM-MAP-RAC/SPA, Proceedings of the First Symposium on the Coralligenous and Other Calcareous Bio-Concretions of the Mediterranean Sea, Tabarka, January 15–16, 2009, pp. 123–128.

Sartoretto, S., Schohn, T., Bianchi, C. N., Morri, C., Garrabou, J., Ballesteros, E., et al. (2017). An Integrated Method to Evaluate and Monitor the Conservation State of Coralligenous Habitats: the INDEX-COR Approach. *Mar. Pollut. Bull.* 120, 222–231. doi:10.1016/j.marpolbul.2017.05.020

Sartoretto, S., Verlaque, M., and Laborel, J. (1996). Age of Settlement and Accumulation Rate of Submarine "coralligène" (−10 to −60 M) of the Northwestern Mediterranean Sea; Relation to Holocene Rise in Sea Level. *Mar. Geol.* 130, 317–331. doi:10.1016/0025-3227(95)00175-1

Titschack, J., Nelson, C. S., Beck, T., Freiwald, A., and Radtke, U. (2008). Sedimentary Evolution of a Late Pleistocene Temperate Red Algal Reef (Coralligène) on Rhodes, Greece: Correlation with Global Sea-Level Fluctuations. *Sedimentology* 55, 1747–1776. doi:10.1111/j.1365-3091.2008.00966.x

UNEP-MAP-RAC/SPA (2008). *Action Plan for the Conservation of the Coralligenous and Other Calcareous Bio-Concretions in the Mediterranean Sea*. Tunis: Rac/Spa, 1–21.

UNEP-MAP-RAC/SPA (2017). *Action Plan for the Conservation of the Coralligenous and Other Calcareous Bio-Concretions in the Mediterranean Sea*. Athens, Greece: Rac/Spa, 1–20.

Zapata-Ramírez, P. A., Scaradozzi, D., Scaradozzi, D., Sorbi, L., Palma, M., Pantaleo, U., et al. (2013). Innovative Study Methods for the Mediterranean Coralligenous Habitats. *Adv. Oceanogr. Limnol.* 4 (2), 102–119. doi:10.1080/19475721.2013.849758